Okada N, Fukagawa K, Takano Y, Dogru M, **Tsubota K**, Fujishima H, Matsumoto K, Nakajima T, Saito H.	The implications of the upregulation of ICAM-1/VCAM-1 expression of corneal fibroblasts on the pathogenesis of allergic keratopathy.	**Invest Ophthalmol Vis Sci**	46(12)	4512-4518	2005
Onguchi T, Takano Y, Dogru M, **Tsubota K**, Shimazaki J.	Clinical evaluation of the accuracy of intraocular pressure measurement by Tono-Pen XL in eyes with amniotic membrane patching.	**Am J Ophthalmol**	139(3)	570-571	2005
Shimmura S, Miyashita H, Konomi K, Shinozaki N, Taguchi T, Kobayashi H, Shimazaki J, Tanaka J, **Tsubota K**.	Transplantation of corneal endothelium with Descemet's membrane using a hyroxyethyl methacrylate polymer as a carrier.	**Br J Ophthalmol**	89(2)	134-137	2005
Shimmura S, Shimazaki J, Omoto M, Teruya A, Ishioka M, **Tsubota K**.	Deep lamellar keratoplasty (DLKP) in keratoconus patients using viscoadaptive viscoelastics.	**Cornea**	24(2)	178-181	2005
Shiraishi K, Tsuzaka K, Yoshimoto K, Kumazawa C, Nozaki K, Abe T, **Tsubota K**, Takeuchi T.	Critical role of the fifth domain of E-cadherin for heterophilic adhesion with alphaEbeta7, but not for homophilic adhesion.	**J Immunol**	175(2)	1014-1021	2005
Takahashi Y, Igaki M, Suzuki A, Takahashi G, Dogru M, **Tsubota K**.	The effect of periocular warming on accommodation.	**Ophthalmology**	112(6)	1113-1118	2005
Yamada M, Mochizuki H, Kawai M, **Tsubota K**, Bryce TJ.	Decreased tear lipocalin concentration in patients with meibomian gland dysfunction.	**Br J Ophthalmol.**	89(7)	803-805	2005

Yoshida S, Shimmura S, Shimazaki J, Shinozaki N, **Tsubota K**.	Serum-free spheroid culture of mouse corneal keratocytes.	**Invest Ophthalmol Vis Sci**	46(5)	1653-1658	2005
Atsuko Toshino, Atsushi Shiraishi, Atsushi Suzuki, Wei Zhang, Toshio Kodama **Yuichi Ohashi**	Expression of keratinocyte transglutaminase in cornea of vitamin A-deficient rats.	**Curr Eye Res**	30	731-739	2005
Atsuko Toshino, Toshihiko Uno , **Yuichi Ohashi** , Naoyuki Maeda, Tetsuro Oshika	Transient keratectasia caused by intraocular pressure elevation after laser in sutu keratomileusis.	**J Cataract Refract Surg**	31	200-204	2005
Takashi Suzuki, Yoshiaki Kawamura, Toshihiko Uno, **Yuichi Ohashi,** Takayuki Ezaki	Prevalence of Staphylococcus epidermidis strains with biofilm-forming ability in isolates from conjunctiva and facial skin.	**Am J Ophthalmol**	40	844-850	2005

An Investigation into the Composition of Amniotic Membrane Used for Ocular Surface Reconstruction

Leanne J. Cooper, PhD, Shigeru Kinoshita, MD, PhD,† Matthew German, PhD,* Noriko Koizumi, MD, PhD,† Takahiro Nakamura, MD, PhD,† and Nigel J. Fullwood, PhD**

Purpose: Cultivated limbal epithelial transplantation using an amniotic membrane (AM) carrier is now widely used for ocular surface reconstruction. The reasons for the exceptional success of AM as a carrier are not fully understood but are believed to be related to its unique composition. In this project we characterize, at the ultrastructural level, the extracellular matrix (ECM) components present in AM. We also compare the distribution of ECM components of cellular AM with that of denuded AM.

Methods: Scanning, transmission, and atomic force microscopy was used to examine the structure of cellular and denuded amniotic membranes. Immunogold labeling with a panel of antibodies against ECM molecules was carried out on cellular and denuded AM.

Results: Heparan sulfate, fibronectin, and laminin were present at high concentration in the lamina densa, Collagen IV was the major component of the basal lamina. Type I collagen was confined to the stroma along with significant amounts of keratan and chondroitin sulfate. Both cellular and denuded AMs had similar distributions of the ECM components.

Conclusions: We were able to determine the distribution of ECM molecules in the lamina densa, basal lamina, and stroma of AM at the ultrastructural level. The removal of amniotic epithelial cells using our protocol does not appear to have any significant effects on the structure of the basal lamina or the distribution of ECM components.

Key Words: amniotic membrane, basal lamina, extracellular matrix

(*Cornea* 2005;24:722–729)

Human amniotic membrane (AM) has been used in various surgical procedures to promote epithelialization and prevent tissue adhesion. In the last few years the benefits of using AM transplantation in conjunction with limbal grafting have been demonstrated.[1–5] The exact reasons why AM is so beneficial in ocular surface reconstruction is not yet fully understood. Evidence shows that AM facilitates rapid re-epithelialization, promotes cellular differentiation,[6] and suppresses inflammation and vascularization.[7]

The human amnion is the innermost layer of the placenta and is composed of a single epithelial layer, a thick basal lamina and an avascular stroma. The apical surface of the basal lamina also has a thin electron-dense layer termed the lamina densa to which the base of the epithelial cells attaches, which is only visible with the electron microscope. The extracellular matrix (ECM) components of the AM basal lamina have been characterized at the light microscope level[8,9]; however, the light microscope is not able to distinguish between the basal lamina and lamina densa. The lamina densa is only 10–20 nm thick, is in direct contact with the epithelial cells, and is the layer most likely to be damaged if the AM is denuded of cells before use.

Although previous workers have investigated basement membrane components in AM, its composition has never fully been investigated at the ultrastructural level, in particular the lamina densa, which plays vital roles in cell adhesion, cell migration, proliferation, and differentiation of the corneal epithelium. To increase our understanding of the mechanisms by which AM confers its beneficial effects, it is particularly important to know which ECM molecules come into direct contact with basal epithelial cells, eg, those in the lamina densa region.

In this paper we have used a panel of antibodies directed to a variety of extracellular matrix proteins to determine the composition of the extracellular matrix of AM to a resolution of a few nanometers.

There is currently some discussion as to whether the cellular or the acellular (denuded form) AM is a better substrate for the ex vivo expansion of corneal epithelial stem cells for ocular surface reconstruction. Some workers have reported the potential benefits of the intact cellular form. For example, it has been shown that amniotic epithelial cells produce neurotransmitters,[10] neuropeptides, neurotrophic factors,[11,12] and, recently, pigment-derived growth factor (PEDF),[13] all of which may potentially support the growth and function of corneal epithelial cells in a culture system. Greuterich et al have reported the advantages of using an intact cellular form of AM.[14] In contrast to this, other groups have reported that the best results are obtained with the denuded form.[15] However, some workers have expressed concern as to whether the denuding process, which removes cells from the AM, could result in the loss of

Received for publication May 27, 2004; revision received October 21, 2004; accepted November 5, 2004.

From the *Institute of Environmental and Natural Sciences, Lancaster University, Lancaster LA1 4YQ, United Kingdom; and †Department of Ophthalmology, Kyoto Prefectural University of Medicine, Kyoto, Japan.

Supported by grants from the Japanese Ministry of Health and Welfare and the Japanese Ministry of Education, Tokyo, the Kyoto Foundation for the Promotion of Medical Science, the Intramural Research Fund of the Kyoto Prefectural University of Medicine, the EPSRC, and the Wellcome Trust.

Reprints: Nigel J. Fullwood, PhD, Institute of Environmental and Natural Sciences, Lancaster University, Lancaster LA1 4YQ, UK.

ECM components or damage the basal lamina. Therefore, a second objective of this study was to compare the distribution of ECM components in cellular and denuded AM to determine if the denuding process results in changes to the ECM composition of the AM. Particular attention was paid to the lamina densa because this is the most apical and most easily damaged component of the basal lamina.

MATERIALS AND METHODS

Preparation of Amniotic Membrane

In accordance with the tenets of the Declaration of Helsinki and with proper informed consent, human AMs were obtained at the time of cesarean section. The membranes were washed with sterile phosphate-buffered saline (PBS) containing antibiotics (5 mL of 0.3% ofloxacin) under sterile conditions. The AM was washed 3 more times with sterile PBS and cut into pieces approximately 2.5 cm × 2.5 cm in size. The samples were divided into 2 groups, cellular and denuded. For the denuded samples, membranes were deprived of their amniotic epithelial cells by incubation with 0.02% ethylene diamine tetraacetic acid (EDTA, Waco Pure Chemical Industries, Osaka, Japan) at 37°C for 2 hours to loosen cellular adhesion, followed by gentle scraping using a cell scraper[15] (Nalge Nunc International, Naperville, IL). Both AMs were then stored at −80°C in Dulbecco Modified Eagle Medium (Gibco BRL, Rockville, MD) and glycerol (Nacalai Tesqu Co, Kyoto, Japan) at the ratio of 1:1 (vol/vol).

Scanning Electron Microscopy

Frozen amniotic membranes were thawed at room temperature for 10 minutes. The samples were then fixed in 4% glutaraldehyde in PBS for 2 hours. They were washed in PBS for 15 minutes and then postfixed in 2% osmium tetroxide for 2 hours. They were washed again in PBS before being passed through an alcohol series. After two 20 minute changes of 100% ethanol, the samples were then transferred to hexamethyldilisane for 10 minutes and air dried. The samples were then mounted on aluminum specimen stubs and sputter coated with gold before being examined on a JEOL JSM 5600 scanning electron microscope.

Transmission Electron Microscopy

Frozen amniotic membranes were thawed at room temperature for 10 minutes. The samples were then fixed in 4% glutaraldehyde in PBS for 2 hours. They were washed in PBS for 15 minutes and then postfixed in 2% osmium tetroxide for 2 hours. They were washed again in PBS before being passed through an alcohol series and embedded in araldite resin (Agar Scientific, UK). Ultrathin sections were cut on a Reichert Ultracut E, collected on naked copper grids, and stained with aqueous uranyl acetate, phosphotungstic acid, and lead citrate before being examined on a JEOL JEM 10-10 transmission electron microscope.

Atomic Force Microscopy

Samples of AM were removed from the buffer solution and cut to produce a specimen approximately 3 mm^2. The specimen was then placed onto freshly cleaved mica mounted on a 5-mm-diameter metallic disk and allowed to air dry at ambient temperature. The specimens were then stored in a desiccator until required for imaging. All of the images were obtained with a Digital Instruments Multimode™ AFM (Veeco, Cambridge, UK) in conjunction with a Nanoscope IIIa controller using Si_3N_4 cantilever probes (TESP, Veeco). The dehydrated AM specimens were imaged in air using the tapping mode™.

Transmission Electron Microscopy Immunogold Labeling

Frozen amniotic membranes were thawed at room temperature for 10 minutes and washed in PBS. They were dehydrated through a graded alcohol series to 90% and embedded in LR white resin (TAAB Laboratories, Berkshire, UK). Ultrathin sections were cut on an ultramicrotome and collected on gilded copper grids. Grids were placed in droplets of 0.1 M glycine in PBS for 2 times 10 minutes and in normal goat serum for 20 minutes. Grids were incubated overnight at 4°C in a grid box loaded with 15μl of primary antibody diluted with PBS buffer at pH 7.4 containing 1% bovine serum albumin (BSA) and 1% Tween 20. Grids were washed 5 times in buffer 1 for 8 minutes each and then 5 times in distilled water for 8 minutes. Grids were then incubated for 3 hours at room temperature with 15 μL of the appropriate 5-nm gold-conjugated secondary antibody diluted with PBS at pH 8.2 containing 1% BSA, 1% Tween 20, 1% normal goat serum, 1% fish gelatin, and 2% sodium chloride. Specimens were washed 5 times in buffer 2 for 8 minutes each and then 5 times in distilled water for 8 minutes. Sections were counterstained in aqueous uranyl acetate for 30 minutes before being examined on a JEOL 10-10 transmission electron microscope.

Antibodies

Primaries

1. Anti–collagen type IV, NLI/53 (Biogenesis Ltd). Reactive with native and denatured forms of type IV collagen. Does not cross-react with types II, III, V, or I.
2. Anti–collagen type I, Col 1 (Sigma Chemical Co.), mouse monoclonal (in ascites) Isotype IgG1. Recognizes the native (helical) form of collagen type I. No cross-reactivity with types II, III, IV, V, VI, VII, IX, X, or XI.
3. Antilaminin (Sigma Chemical Co.), affinity-isolated antigen-specific antibody, developed in rabbit. No reaction with fibronectin, vitronectin collagen type IV, or chondroitin sulfate types A, B, or C.
4. Antifibronectin (Sigma Chemical Co.), affinity-isolated antigen-specific antibody (IgG) developed in rabbit. Immunospecific for human fibronectin. No reaction with collagen type IV, laminin, vitronectin, and chondroitin sulfate types A, B, or C.
5. Anti–keratan sulfate, 1/20/5-D-4 (ICN Biochemicals Ltd.), recognizes hepta- or larger oligosaccharides of the poly (*N*-acetyllactosamine) series.
6. Anti–heparan sulfate, F58-10E4 (Seikagaku Corporation), recognizes 1 or more *N*-sulfated glucosamine residue(s).
7. Anti–chondroitin sulfate, CS-56 (Sigma Chemical Co.), recognizes an epitope present in native chondroitin 4- and chondroitin 6-sulfate chains.

Controls

The primary antibody was replaced with a negative control IgG or IgM antibody (Serotec, Oxford, UK) at an equivalent dilution. These antibodies are especially produced to act as controls for immunohistochemisty and show the level of non-specific isotype matched IgG and IgM binding to the sections.

Secondaries

Secondary antibodies, goat anti-mouse or anti-rabbit IgG or IgM, conjugated to 5-nm gold (British Biocell International), were used to visualize the primary antibody in the transmission electron microscope.

RESULTS

Scanning Electron Microscopy

Examination of the apical surface of cellular amniotic membrane showed a continuous layer of polygonal epithelial cells. The cell junctions were distinct, and the surface of the cells was covered with numerous microvilli (Fig. 1A). Examination of the denuded amniotic membrane after EDTA treatment and cell scraping confirmed that the amniotic membrane epithelial cells had been removed, leaving a smooth nonfibrillar surface and indicating that the basal lamina is still intact (Fig. 1B).

Transmission Electron Microscopy

Examination of cellular amniotic membrane by transmission electron microscopy showed that the amniotic membrane epithelial cells were attached to the basement membrane region by numerous hemidesmosomal contacts (Fig. 2A). A thin electron-dense layer about 10–20 nm thick can be clearly seen at the apical surface of the basal lamina, just below the basal surface of the epithelial cells; this layer is termed the lamina densa. Below this is the basal lamina, which is 200–300 nm thick and has a fine fibrillar structure. Below the basal lamina is the stroma. The stroma is a few micrometers thick and is composed of collagen fibrils about 30 nm in diameter. The lamina densa, basal lamina, and stroma are also clearly visible on the denuded AM samples (Fig. 2B).

Atomic Force Microscopy

The atomic force microscope showed that the borders of the epithelial cells can be discerned in the cellular AM samples (Fig. 3A). The cell layer appears smoother and the cell junctions less well defined than we see with the SEM, and microvilli are not visible. This is because the glycocalyx layer on the surface of the epithelium is still intact: the sample preparation for AFM does not involve chemical fixatives or solvents. Importantly, examination of the denuded AM surface (Fig. 3B) shows it to be smooth and clearly nonfibrillar in nature. Even in high-resolution mode the AFM showed no evidence of type IV collagen structure, indicating that the lamina densa remains intact on the denuded AM.

Immunogold Labeling

As with all immunolabeling studies the preparation of specimens is a difficult compromise between achieving good structural preservation by the use of powerful chemical fixatives or preservation of the epitopes' antigenicity by avoiding chemical fixatives.[16] Because many of the epitopes labeled in this study were highly sensitive to aldehydes, these had to be avoided, so the quality of structural preservation is much poorer than that seen in the samples prepared for conventional microscopy (Fig. 2). In addition, the sections have not been heavily counterstained in order that the gold particles can be seen clearly above the grain of the stain. Despite these problems, which are inherent to immunolabeling at the electron microscope level, the structural preservation was good enough to allow us to clearly identify the lamina densa, the basal lamina, and the stroma of the AM.

The lamina densa, basal lamina, and stroma of cellular and denuded AM showed similar patterns of labeling for all of the ECM components examined. Labeling for fibronectin was found in the lamina densa (Fig. 4A,B) together with high levels of laminin (Fig. 4C,D). Labeling for collagen type IV was observed within the whole basal lamina region including the lamina densa (Fig. 4E,F). Collagen type I labeling was found only in the stroma region of both cellular and denuded samples; the labeling was associated with the collagen fibrils (Fig. 4G,H).

Labeling for keratan sulfate (KS) was found in the stroma region of cellular and denuded AMs generally between the collagen fibrils (Fig. 5A,B). A similar pattern of labeling was observed for chondroitin sulfate (CS) (Fig. 5C,D). In contrast, labeling for heparan sulfate (HS) was found only in the lamina densa, where the labeling was quite intense (Fig. 5E,F). Immunolabeling with the control nonspecific antibody showed negligible levels of reactivity in both samples (Fig. 5G,H).

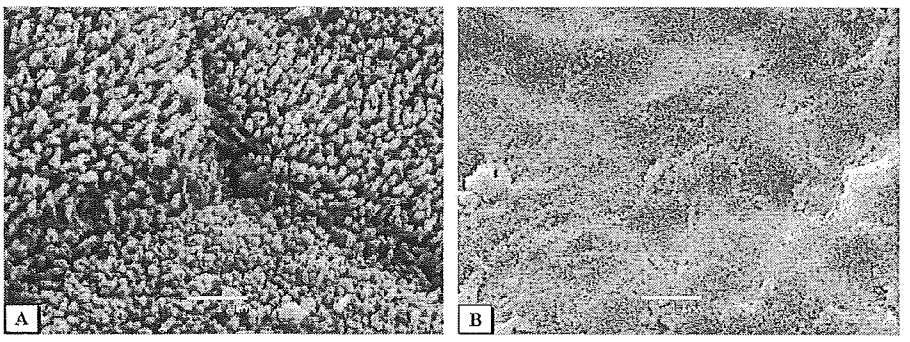

FIGURE 1. Scanning electron micrographs of cellular (A) and denuded (B) amniotic membrane. (A) The micrograph shows the junctions among 3 cells. The cell junctions are well defined, and the cell surface is covered with numerous microvilli. (B) In the denuded AM it is clear that all the amniotic epithelial cells have been removed from this region, and the basement membrane is visible. The smooth nonfibrillar surface indicates that the lamina densa is still intact.

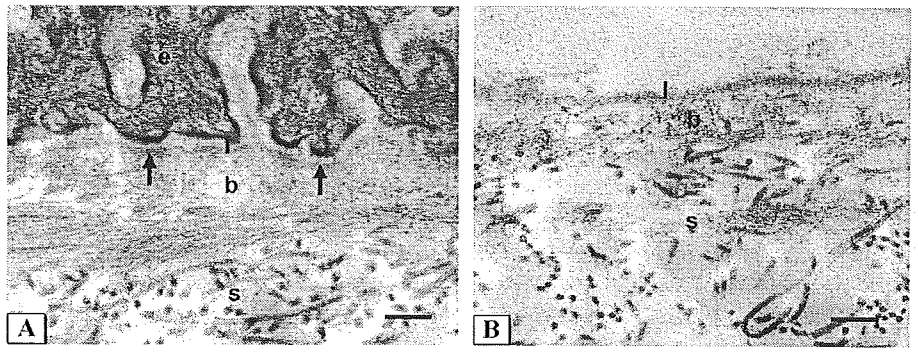

FIGURE 2. Transmission electron micrographs of cellular (A) and denuded (B) amniotic membrane. (A) Amniotic membrane epithelial cells (e) are attached to the basal lamina by hemidesmosomal junctions (arrows). In both samples, the lamina densa (l), the basal lamina (b), and the stroma (s) are clearly visible (scale bars, 200 nm).

DISCUSSION

The extracellular matrix (ECM) molecules within any basement membrane have a huge influence on the adhesion and growth of the overlying cells. As well as allowing the cells to attach and migrate, the ECM molecules can also transmit signals via their interactions with integrins. The engagement of an integrin with an ECM molecule can induce a variety of responses within a cell, including changes in cytoplasm pH, calcium ion concentration, protein phosphorlylation, and gene expression. These changes in turn can influence the cell's state of differentiation, its migratory activity, and its growth potential. Although previous studies have reported on the distribution of some ECM components in AM at the light microscope level,[8] a comprehensive survey of their distribution at the ultrastructual level has not yet been carried out. Immunolabeling at the electron microscope level allows us to localize the ECM molecule to within a few nanometers and therefore makes it possible to discriminate among different regions of the basement membrane. It is of particular importance that we are able to determine which molecules will come within direct contact with the epithelial cells, ie, those in the lamina densa, which is visible only with the electron microscope.

The results of this investigation into the distribution of ECM components in AM at the ultrastructural level should help us to understand why the AM supports corneal epithelial stem cell adhesion, migration, and proliferation so well. This will provide insight into the fundamental mechanisms of corneal epithelial adhesion, migration, and proliferation. This information is of potential use in the design of a synthetic version of the AM. Although the amniotic membrane is a very effective carrier for corneal stem transplantation, it has one potential drawback: a theoretical risk for the transmission of unknown viral or prion agents to the recipient; because of this, attempts are already being made to produce a synthetic version of this membrane. Clearly, a thorough understanding of the ECM composition of the AM would help in the design and production of artificial corneal epithelial carriers or for the modification of the anterior surfaces of keratoprostheses to encourage reepithelialization after implantation.

Our ultrastructural investigation shows, as would be expected, that the extracellular component of the basement membrane can be divided into the stroma several micrometers thick consisting of fibrillar collagen fibrils 30–40 nm in diameter in a disorganized arrangement. Above this is the

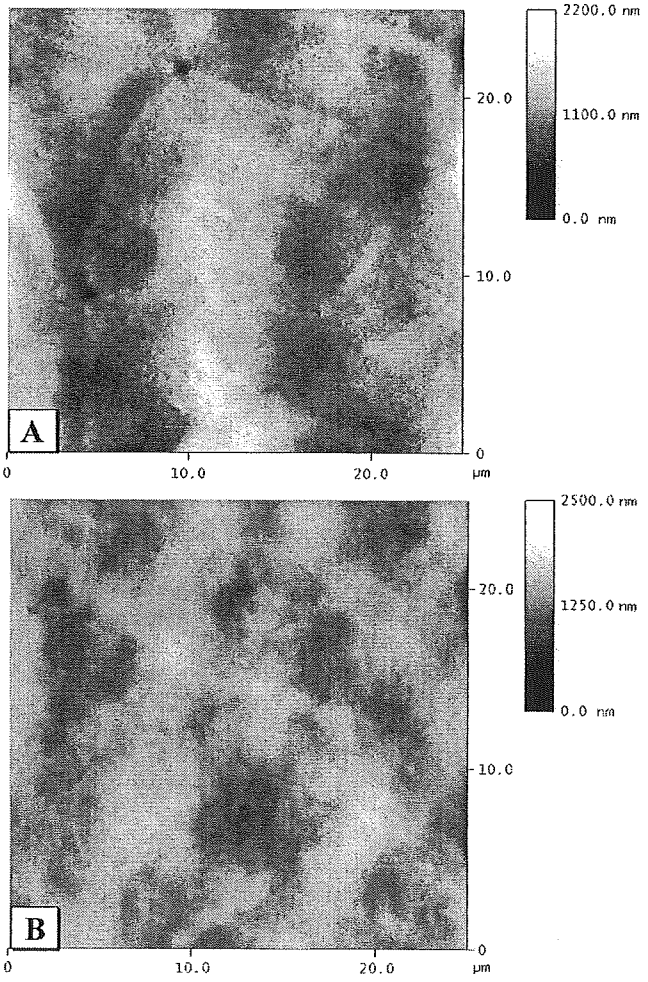

FIGURE 3. Atomic force micrographs of cellular (A) and denuded (B) amniotic membrane. The bar provides information on the height of features on the micrographs. The image of cellular AM allows the outline of an epithelial cell to be made out, but the cell junctions are much less distinct than in Fig. 2A, and no microvilli are visible. This is because the glycocalyx layer is still intact. (B) The surface of the denuded AM appears smooth and featureless, indicating that the lamina densa is still intact. Scan size 25 × 25 μm.

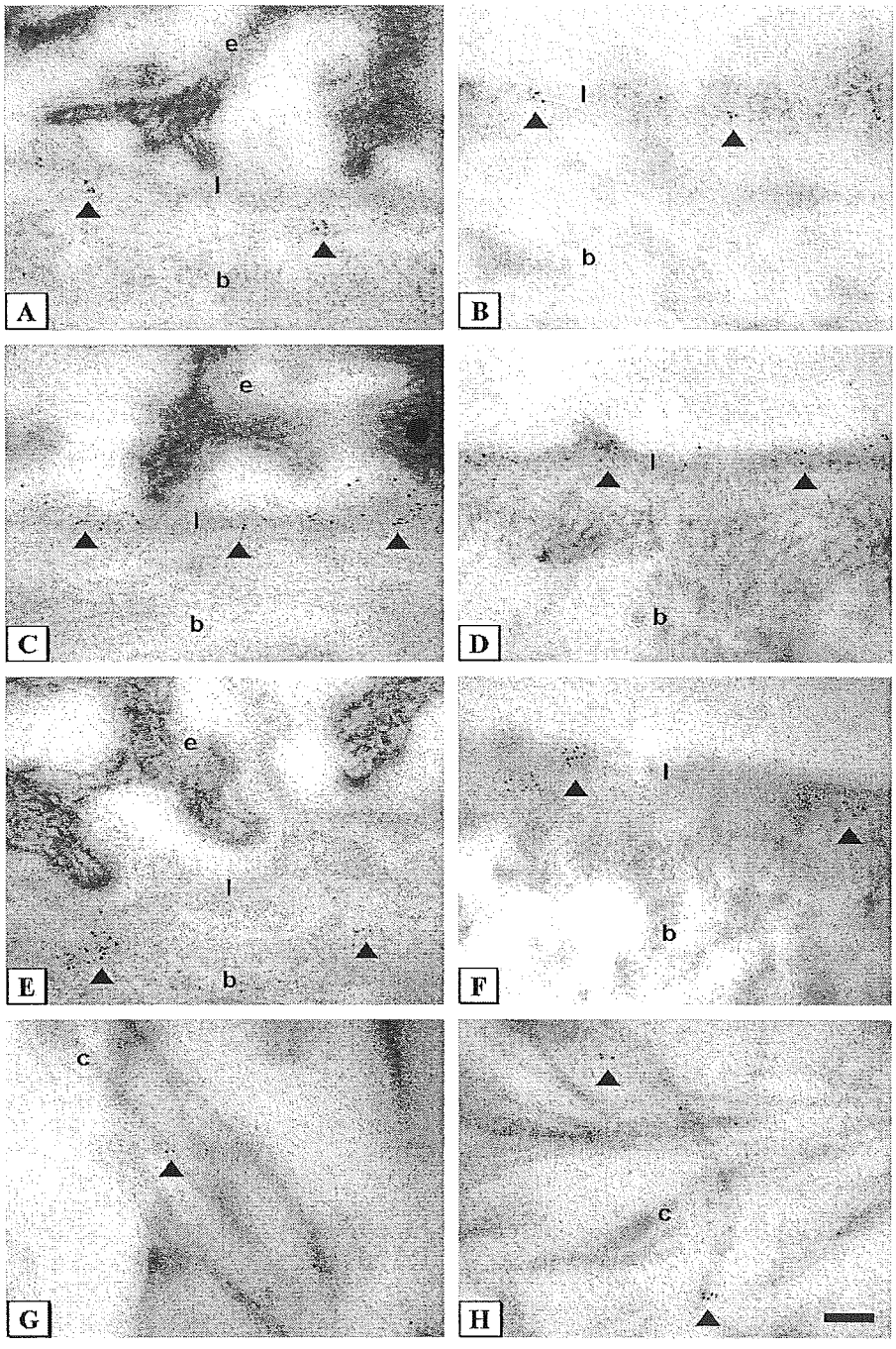

FIGURE 4. Transmission electron micrographs of cellular (A, C, E, and G) and denuded (B, D, F, and H) amniotic membrane. The pattern of immunolabeling was similar in cellular and denuded amniotic membrane. The 5-nm gold particles appear as black dots indicated by arrowheads. Immunolabeling for fibronectin showed moderate levels of staining in the lamina densa of cellular and denuded AMs (A and B). High levels of labeling with laminin were found in the lamina densa region in both samples (C and D). Type IV collagen was located in clusters along the basement membrane in cellular and denuded samples (E and F). Type I collagen was closely associated with collagen fibrils (G and H). Epithelial cell (e), lamina densa (l), basal lamina (b), collagen fibrils (c) (scale bars, 100 nm).

basal lamina, about 200–300 nm thick, composed of fine fibrils a few nanometers in diameter. At the apical surface of the basement membrane is the lamina densa, an electron-dense layer just 10–20 nm thick.

The results of our investigation on cellular AM reveal that fibronectin and laminin are concentrated mostly in the lamina densa. This is the part of the basement membrane directly below the cells and in direct contact with the base of the cells. Both fibronectin and laminin are adhesive glycoprotiens, molecules that have multiple binding sites both to the cells and to the ECM molecules. Heparan sulfate was also detected within the lamina densa in quite large amounts. It is very likely that the HS detected forms part of the proteoglycan perlecan, which is an important component of basement membranes. The HS proteoglycan perlecan has been localized to the basement membrane region in corneal epithelium.[8,17] Perlecan is involved in binding of growth factors and interaction with various extracellular proteins and cell adhesion

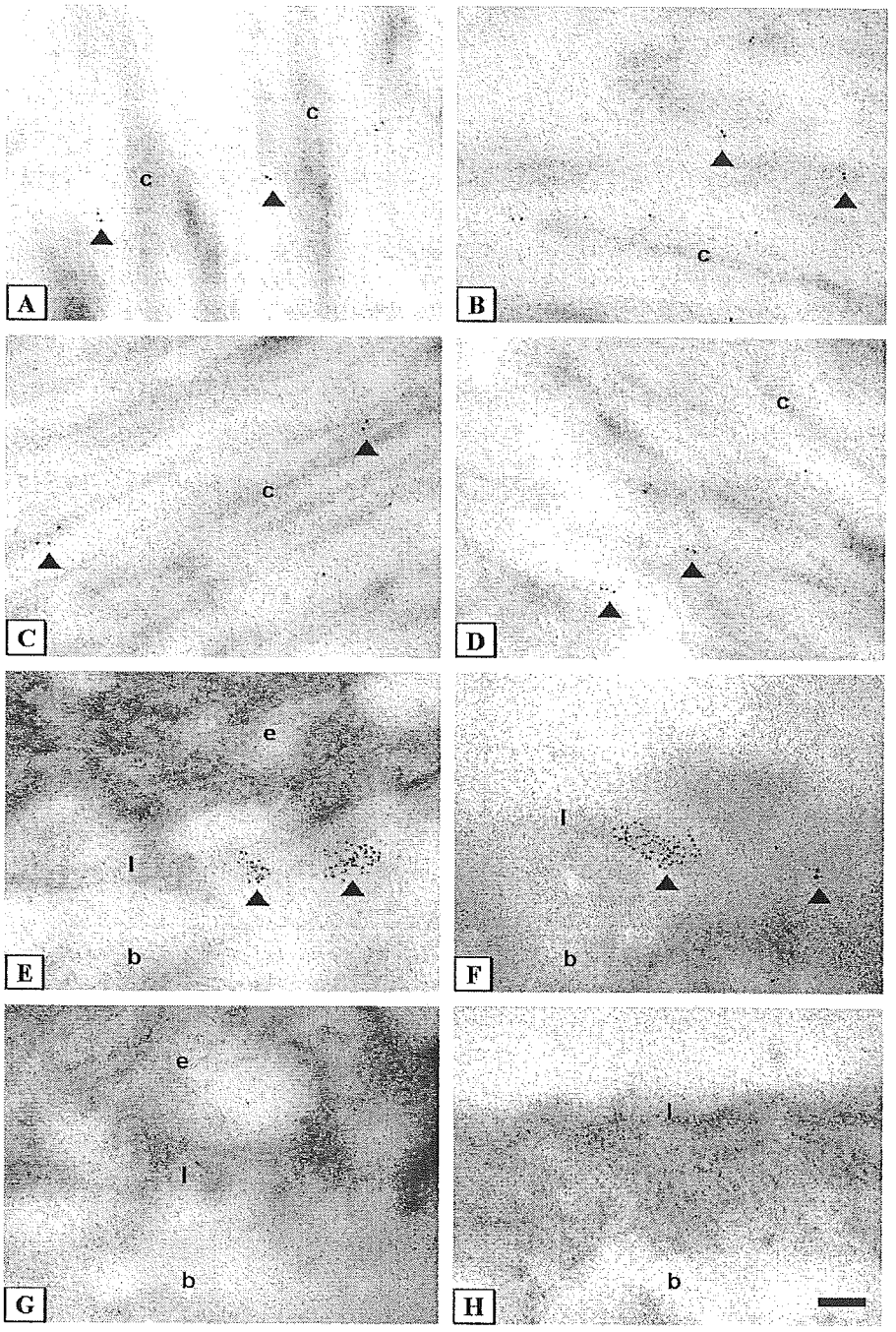

FIGURE 5. Transmission electron micrographs of cellular (A, C, E, and G) and denuded (B, D, F, and H) amniotic membrane. The pattern of immunolabeling was similar in cellular and denuded amniotic membrane. The 5-nm gold particles appear as black dots indicated by arrowheads. Immunolabeling for KS and CS showed similar distribution with labeling in close proximity to collagen fibrils in cellular and denuded AMs (A, B, C, and D). In contrast, labeling for HS was localized to specific regions of the basement membrane in both samples (E and F). Labeling with the nonspecific control antibody showed negligible levels of reactivity (G and H). Epithelial cell (e), lamina densa (l), basal lamina (b), and collagen fibrils (c) are shown (scale bars, 100 nm).

molecules.[18] The role of perlecan in cell adhesion and its increased production and deposition by corneal epithelial cells in culture suggest that HS is important to the formation of the basal lamina and in the adherence of corneal epithelial cells to AM during cultivation.

Our immunolabeling results show that the makeup of the lamina densa of the AM is basically very similar in ECM composition to the lamina densa of the corneal epithelium lamina at the apical surface of the Bowman layer.[19] Because of this similarity, it is not surprising that the corneal epithelial cells adhere to, migrate, and proliferate so well on the lamina densa of the AM.

Below the lamina densa the majority of the basal lamina is made up of type IV collagen. We also found some labeling for HS and laminin in this region. Perlecan is known to interact with type IV collagen and laminin has binding sites for both type IV collagen and perlecan. The interactions between these components stabilize the whole basal lamina.

Below the basal lamina is the AM stroma. The collagen fibrils here labeled strongly for type I collagen as would be

expected. We also found significant labeling for KS and CS in the AM stroma. It has previously been shown that CS is a major component present in the human amnion of pregnant women.[20] The immunogold labeling for KS and CS was often localized on the collagen fibrils. KS and CS proteoglycans are both known to have a role in the organization of the type I collagen fibrils in the corneal stroma[21] and are also found interacting with type I collagen fibrils in the Bowman layer.[19] Again, the arrangement of type I collagen fibrils associated with KS and CS proteoglycans is remarkably similar to the make up of Bowman layer[19] and might account for the reason that the AM readily adheres and eventually integrates onto the corneal surface. It is conceivable that keratan and chondroitin sulfate proteoglycans, which are associated with the type I collagen fibrils in the AM stroma, can also interact with the type I collagen fibrils in Bowman layer. Recent studies of removed AM transplants have also shown that the AM stroma can become invaded and colonized by corneal keratocytes,[22] which further supports the idea that the stroma of the AM and the stroma of the cornea have a great deal in common.

The ECM composition of the AM lamina densa and that of the lamina densa of the corneal epithelium are very close. In addition, there is similarly between the composition of Bowman layer and the AM stroma. It seems likely that these similarities in composition are what help the AM to provide such a good substrate for the growing corneal epithelium on the anterior surface of the AM and what allow the posterior or stroma surface to adhere to and integrate with the surface of the cornea.

The results of this paper show that we did not find any detectable difference in the distribution of ECM molecules in cellular and denuded AM. This finding is confirmed by transmission electron, scanning electron, and atomic force microscopic comparison of cellular and denuded AM. All of these techniques show that in the denuded AM the lamina densa is still present. In transmission electron microscopy this is visible as a thin dense line about 20 nm in thickness. Although both scanning electron and atomic force microscopy both show that the denuded surface is smooth and nonfibrillar, thus confirming that the smooth lamina densa surface has not been damaged or removed exposing the fine fibrillar type IV collagen below.

Greuterich and co-workers have reported potential advantages using a cellular amniotic membrane for the support of epithelial cell growth.[14] In particular, they showed epithelial stem cells grown on cellular amniotic membrane became less differentiated and retained their stem cell characteristics longer. Furthermore, amniotic cells may have a significant role in supplying cultivated corneal stem cells with neurotransmitters, neuropeptides, neurotrophic factors, and PEDF.[10–13] However, there are a number of potential limitations with using cellular AM. First, the residual amniotic membrane epithelial cells are stored frozen; therefore, the cells are not viable. Thus, any benefits of growing epithelial cells on cellular AM might be quite short term and last only until the nonviable AM cells and cell debris are broken down and lost from the AM.[23,24] Second, it seems reasonable to assume that the nonviable AM cells will not provide a secure anchor for the growing corneal epithelial cells. However, because there is no information as to how long nonviable AM cells remain attached to the basal lamina of the AM, the duration of their influence on corneal epithelial cell growth is not known.

With regard to the use of denuded AM for the support and growth of corneal epithelial cells, this investigation has shown that the basal lamina and lamina densa of the AM are undamaged following removal of amniotic membrane cells using our protocol.

In conclusion, this investigation has shown that the denuded AM is remarkably well suited to its role in supporting the proliferation of corneal epithelial cells, its integration and attachment to the underlying Bowman layer, and its role in providing strength and support. It will probably be some time before we can produce an artificial membrane, which is a satisfactory substitute for AM.

REFERENCES

1. Tsubota K, Satake Y, Ohyama M, et al. Surgical reconstruction of the ocular surface in advanced ocular cicatricial pemphigoid and Stevens-Johnson syndrome. *Am J Ophthalmol.* 1996;122:38–52.
2. Lee SH, Tseng SCG. Amniotic membrane transplantation for persistent epithelial defects with ulceration. *Am J Ophthalmol.* 1997;123:303–312.
3. Prabhasawat P, Barton K, Burkett G, et al. Comparison of conjunctival autografts, amniotic membrane grafts, and primary closure for pterygium excision. *Ophthalmology.* 1997;104:974–985.
4. Shimazaki J, Yang HY, Tsubota K. Amniotic membrane transplantation for ocular surface reconstruction in patients with chemical and thermal burns. *Ophthalmology.* 1997;104:2068–2076.
5. Shimazaki J, Shinozaki N, Tsubota K. Transplantation of amniotic membrane and limbal autograft for patients with recurrent pterygium associated with symblepharon. *Br J Ophthalmol.* 1998;82:235–240.
6. Meller D, Tseng SCG. Conjunctival epithelial cell differentiation on amniotic membrane. *Invest Ophthalmol Vis Sci.* 1999;40:878–886.
7. Chen HJ, Pires RT, Tseng SCG. Amniotic membrane transplantation for severe neurotrophic corneal ulcers. *Br J Ophthalmol.* 2000;84:826–833.
8. Fukuda K, Chikama T, Nakamura M, et al. Differential distribution of subchains of the basement membrane components type IV collagen and laminin among the amniotic membrane, cornea, and conjunctiva. *Cornea.* 1999;18:73–79.
9. Nakamura T, Yoshitani M, Rigby H, et al. Sterilized, freeze-dried amniotic membrane: a useful substrate for ocular surface reconstruction. *Invest Ophthalmol Vis Sci.* 2004;45:93–99.
10. Sakuragawa N, Elwan MA, Uchida S, et al. Non-neuronal neurotransmitters and neurotrophic factors in amniotic epithelial cells: expression and function in humans and monkey. *Jpn J Pharmacol.* 2001; 85:20–23.
11. Uchida S, Inanaga Y, Kobayashi M, et al. Neurotrophic function of conditioned medium from human amniotic epithelial cells. *J Neurosci Res.* 2000;62:585–590.
12. Touhami A, Grueterich M, Tseng SC. The role of NGF signaling in human limbal epithelium expanded by amniotic membrane culture. *Invest Ophthalmol Vis Sci.* 2002;43:987–994.
13. Shao C, Sima J, Zhang SX, et al. Suppression of corneal neovascularization by PEDF release from human amniotic membranes. *Invest Ophthalmol Vis Sci.* 2004;45:1758–1762.
14. Grueterich M, Espana E, Tseng SCG. Connexin 43 expression and proliferation of human limbal epithelium on intact and denuded amniotic membrane. *Invest Ophthalmol Vis Sci.* 2002;43:63–71.
15. Koizumi N, Fullwood NJ, Bairaktaris G, et al. Cultivation of corneal epithelial cells on intact and denuded human amniotic membrane. *Invest Ophthalmol Vis Sci.* 2000;41:2506–2513.
16. Beesley JE. Colloidal Gold: A New Perspective for Cytochemical Marking. Microscopy Handbooks 17. Oxford: Oxford University Press, Royal Microscopical Society, 1989.
17. Ohji M, Sundar Raj N, Hassell JR, et al. Basement membrane synthesis by human corneal epithelial cells in vitro. *Invest Ophthalmol Vis Sci.* 1994; 35:479–485.

18. Murdoch AD, Dodge GR, Cohen I, et al. Primary structure of the human heparan sulfate proteoglycan from basement membrane (HSPG2/perlecan). A chimeric molecule with multiple domains homologous to the low density lipoprotein receptor, laminin, neural cell adhesion molecules, and epidermal growth factor. *J Biol Chem.* 1992;267:8544–8557.
19. Bairaktaris G, Lewis D, Fullwood NJ, et al. An ultrastructural investigation into proteoglycan distribution in human corneas. *Cornea.* 1998; 17:396–402.
20. Skinner SJ, Liggins GC. Glycosaminoglycans and collagen in human amnion from pregnancies with and without premature rupture of the membranes. *J Dev Physiol.* 1981;3:111–121.
21. Meek KM, Fullwood NJ. Corneal and scleral collagens—a microscopist's perspective. *Micron.* 2001;32:261–272.
22. Cooper LJ, Fullwood NJ, Koizumi N, et al. An investigation of removed cultivated epithelial transplants in patients after allocultivated corneal epithelial transplantation. *Cornea.* 2004;23:235–242.
23. Kruse FE, Joussen AM, Rohrschneider K, et al. Cryopreserved human amniotic membrane for ocular surface reconstruction. *Graefes Arch Clin Exp Ophthalmol.* 2000;238:68–75.
24. Zhong Y, Ye W, Shen X, et al. The effect of frozen storage for amniotic membrane ultrastructure. *Yan Ke Xue Bao.* 2001;17:202–205, 216.

Available online at www.sciencedirect.com
SCIENCE DIRECT®
ELSEVIER
Biochemical and Biophysical Research Communications 331 (2005) 285–294
BBRC
www.elsevier.com/locate/ybbrc

Triggering of TLR3 by polyI:C in human corneal epithelial cells to induce inflammatory cytokines

Mayumi Ueta [a,*], Junji Hamuro [a], Hiroshi Kiyono [b], Shigeru Kinoshita [a]

[a] *Department of Ophthalmology, Kyoto Prefectural University of Medicine, Kyoto, Japan*
[b] *Division of Mucosal Immunology, The Institute of Medical Science, The University of Tokyo, 4-6-1 Shirokanedai, Minato-ku, Tokyo, Japan*

Received 23 February 2005
Available online 1 April 2005

Abstract

Epithelial cells of the ocular surface are key in the first-line defense as a part of the mucosal immune system against pathogens. We investigated whether polyI:C induces the production by human corneal epithelial cells (HCEC) of pro-inflammatory cytokines and IFN-β, and whether Toll-like receptor (TLR)-3 expression is amplified by polyI:C. TLR3 was expressed on the surface of HCEC. Stimulation with polyI:C elicited the elevated production and mRNA expression of IL-6 and IL-8 in HCEC. While polyI:C induced IFN-β, far stronger than human fibroblasts, and TLR3 gene expression in HCEC, LPS stimulation did not. Similarly, polyI:C, but not LPS, induced the gene expression of IκBα and MAIL, members of the IκB family, in HCEC. The innate immune response of HCEC is distinct from that of immune-competent cells, and we suggest that this is indicative of the symbiotic relationship between corneal epithelium and microbes inhabiting the ocular surface.

Keywords: Human corneal epithelial cells; PolyI:C; TLRs; Inflammation; LPS

On the ocular surfaces as in the intestine, the surface epithelium serves a critical function in the front-line defense of the mucosal innate immune system [1–3]. Upon challenge, epithelial cells lining mucosal surfaces play a pivotal role in innate immunity by secreting chemokines and other immune mediators. The ability to detect microbes is arguably the most important task of the immune system. Exaggerated host defense reaction of the epithelium to endogenous bacteria may induce the initiation and perpetuation of inflammatory mucosal responses [4–6].

The ability of cells to recognize microbial motifs and pathogen associated molecular patterns (PAMPs) rests on pattern recognition receptors (PRRs) [7–9]. Signal transduction depends on the expression of a family of type I transmembrane receptors, Toll-like receptors (TLRs). To date, 11 TLRs have been identified in humans; they are expressed primarily on cell types that are mammalian host immune-competent cells such as dendritic cells and macrophages. These are the cells that are most likely to come into direct contact, via the mucosal epithelia, with pathogens from the environment [10]. TLR expression is not restricted to phagocytic cell types, rather, it appears that the majority of cells in the body including mucosal epithelial cells express at least a subset of TLRs [11]. Some PRRs are located on the cell membrane and respond to extracellular PAMPs; others exist in the cytosol and respond to PAMPs that cross the plasma membrane [12–14]. Signaling through TLRs results in the activation of IKK, NF-κB, and NF-κB target genes, and the coordinated activation of several transcription factors that regulate the expression of antimicrobial genes, cytokines, chemokines, and co-stimulatory molecules [7–9].

* Corresponding author. Fax: +81 75 251 5663.
E-mail address: mueta@ophth.kpu-m.ac.jp (M. Ueta).

0006-291X/$ - see front matter © 2005 Elsevier Inc. All rights reserved.
doi:10.1016/j.bbrc.2005.02.196

Although the eye is relatively impermeable to microorganisms [1,3,15,16], if corneal integrity is compromised by trauma or contact lens wear, sight-threatening bacterial infection may occur [17,18]. Uniquely, human corneal epithelial cells (HCEC) are in constant contact with bacteria and bacterial products; they form a structural and functional barrier against numerous bacteria both pathogenic and nonpathogenic. Factors normally pro-inflammatory for other cell types do not induce epithelial cells to initiate a defensive response [19]. This is especially important with respect to the epithelial cells of the avascular and transparent cornea, where the formation of scar tissue in response to a host inflammatory reaction results in opacification and loss of vision. We previously reported that human corneal epithelial cells failed to respond functionally to PAMPs such as peptidoglycan (PGN) and lipopolysaccharide (LPS) because they lack TLR2 and TLR4 on their surface [20]. Despite the existence of TLR2 and TLR4 in the cytoplasm of HCEC, the experimental translocation of LPS to the cytoplasm did not elicit an immune response [20].

Among the TLRs, TLR4 which recognizes LPS, and TLR3 which recognizes the viral double-stranded RNA-mimic polyI:C have received the greatest attention [21–23]. TLR3-mediated responses are unique because TLR3 activation elicits lower levels of inflammatory cytokines than the activation of other TLR family members, although TLR3 activation induces the very robust secretion of IFN-β [21]. The remarkable similarities in the cellular responses to bacterial and viral infection after pathogen recognition are indicative of cross-talk between virus- and bacteria-induced signaling [24]. Although there were two reports by the same group describing the inhibitory effect of polyI:C against herpetic keratitis in rabbits, nothing is yet known on the reproducibility of their experiments or the effect on the innate immune response [25,26].

Here we demonstrate that HCEC express TLR3 at the cell surface and thus respond to polyI:C to generate pro-inflammatory cytokines and IFN-β. We also show that the surface expression of TLR3 on HCEC was amplified in an autocrine/paracrine manner by polyI:C.

Materials and methods

All experimental procedures were conducted in accordance with the principles set forth in the Helsinki Declaration. The purpose of the research and the experimental protocols were explained to all participants and their prior written informed consent was obtained.

Human corneal epithelial cells. For RT-PCR, human corneal epithelial cells (HCEC) were obtained from corneal buttons of patients undergoing corneal transplantation for early-stage bullous keratopathy (one eye) or keratoconus (two eyes) at the affiliated hospital of Kyoto Prefectural University of Medicine.

Primary HCEC, obtained from Kurabo (Osaka, Japan), were cultured at 37 °C under 95% humidity and 5% CO_2 in serum-free medium consisting of EpiLife (Kurabo) supplemented with HCEC growth supplement (HCGS) containing 1 ng/ml murine epidermal growth factor (mEGF), 5 μg/ml insulin from bovine pancreas, 0.18 μg/ml hydrocortisone, and 0.4% v/v bovine pituitary extract (Kurabo), 0.2% PSA solution, and antibiotic–antimycotic solution (5000 U/ml penicillin, 50 mg/ml streptomycin, and 12.5 μg/ml amphotericin B) (Kurabo) [20]. For assays, 2×10^6 primary HCEC were plated in 25 cm^2 flasks. After reaching sub-confluence, they were either left untreated, exposed to 1 μg/ml LPS from *Pseudomonas aeruginosa* (Sigma, St. Louis, MO), or exposed to 25 μg/ml polyI:C (Invivogen, San Diego, CA) for 1-, 3- or 6 h. The culture time of polyI:C-treated cells was adjusted to be optimal for the maximum induction of IL-6, IFN-β, IκBα, MAIL, and TLR3, it was 6 h for IL-6, IL-8, and TLR3, and 3 h for IFN-β, IκBα, and MAIL.

Purification of human peripheral mononuclear cells. Venous blood samples from healthy volunteers were anti-coagulated with 2Na-EDTA, placed in sterile 50-ml polypropylene tubes, mixed with 1 volume of Ca^{2+}-free PBS (PBS(−)), overlaid with Ficoll–Paque Plus (Amersham Biosciences AB, Uppsala, Sweden), and centrifuged for 20 min at 2000 rpm at 20 °C. Human peripheral mononuclear cells (HPMC) were gently aspirated from the interface and washed with PBS(−). For stimulation with LPS or polyI:C, isolated HPMC were cultured for 1-, 3- or 6 h in RPMI medium (Gibco-BRL Life Technologies, Paisley, UK) supplemented with 10% fetal calf serum (Gibco) and 1% antibiotic–antimycotic solution (100 U/ml penicillin, 100 mg/ml streptomycin, and 250 ng/ml amphotericin B) (Gibco).

Human conjunctival fibroblasts. Human conjunctival fibroblasts (HCFB) were obtained from redundant subconjunctival tissues of patients undergoing cataract surgery at the affiliated hospital of Kyoto Prefectural University of Medicine. Primary HCFB were cultured in DMEM (Gibco) supplemented with 10% fetal calf serum (Gibco) and 1% antibiotic–antimycotic solution (100 U/ml penicillin, 100 mg/ml streptomycin, and 250 ng/ml amphotericin B) (Gibco). For assays, all procedures were the same as those described above for HCEC.

MRC-5 and HeLa cells. MRC-5 and HeLa, expressing TLR3 on the cell surface and producing IFN-β upon polyI:C stimulation, were the gift of Dr. T. Seya (Hokkaido University). MRC-5, normal human lung fibroblasts, and HeLa cells were maintained in MEM (Gibco) supplemented with 1% antibiotic–antimycotic solution (100 U/ml penicillin, 100 mg/ml streptomycin, and 250 ng/ml amphotericin B) (Gibco), and 10% or 5% fetal calf serum (Gibco). For assays, all procedures were the same as those described above for HCEC.

RT-PCR. Total RNA was isolated from human corneal epithelium and HPMC using Trizol Reagent (Life Technologies, New York, NY) according to the manufacturer's instructions. For the RT reaction, we used the SuperScript Preamplification kit (Invitrogen). PCR amplification was performed with DNA polymerase (Takara; Shiga, Japan) for 38 cycles at 94 °C for 1 min, annealing for 1 min, and 72 °C for 1 min on a commercial PCR machine (GeneAmp; PE Applied Biosystems). The primers we used are listed in Table 1. The integrity of the RNA was assessed by electrophoresis in ethidium bromide-stained 1.5% agarose gels.

Flow cytometric analysis. Human primary corneal epithelial cells were treated with 0.02% EDTA. The cell-surface expression of TLR2, TLR3, and TLR4 was examined by flow cytometry. For TLR3 expression, cells were incubated with mouse anti-human TLR3 monoclonal antibody (mAb; Imgenex, San Diego, CA) or isotype control mouse IgG1 (DakoCytomation, Kyoto, Japan) for 30 min at 4 °C. Alexa Fluor 488 goat anti-mouse IgG (H + L) (Molecular Probes, Eugene, OR) was used as the secondary antibody. For TLR2 and TLR4 expression, cells were incubated for 30 min at 4 °C with PE-conjugated mouse anti-human TLR2 (TL2.1), TLR4 (HTA125) monoclonal antibody (eBioscience, San Diego, CA), or isotype control mouse IgG2a (BD PharMingen). Stained cells were analyzed with a FACSCalibur (Becton–Dickinson, San Jose, CA); data were analyzed using Cellquest software (Becton–Dickinson). Moreover, HCFB, MRC-5, and HeLa were examined for their cell-surface expression of TLR3.

Table 1
The primer list of TLRs

Gene	Accession No.		Primers	Bases	Product size (bp)	Annealing
TLR1	NM003263	Sense	5′-TGCCCTGCCTATATGCAA-3′	(381–398)	555	54
		Anti-sense	5′-GAACACATCGCTGACAACT-3′	(918-936)		
TLR2	XM003304	Sense	5′-GCCAAAGTCTTGATTGATTGG-3′	(1783–1803)	346	52
		Anti-sense	5′-TTGAAGTTCTCCAGCTCCTG-3′	(2110–2129)		
TLR3	NM003265	Sense	5′-CGCCAACTTCACAAGGTA-3′	(277–294)	689	54
		Anti-sense	5′-GGAAGCCAAGCAAAGGAA-3′	(949–966)		
TLR4	XM005336	Sense	5′-TGGATACGTTTCCTTATAAG-3′	(1768–1787)	506	52
		Anti-sense	5′-GAAATGGAGGCACCCCTTC-3′	(2256–2274)		
TLR5	NM003268	Sense	5′-ATCTGACTGCATTAAGGGGAC-3′	(2274–2294)	567	52
		Anti-sense	5′-TTGAGCAAAGCATTCTGCAC-3′	(2822–2841)		
TLR6	NM006068	Sense	5′-CCTCAACCACATAGAAACGAC-3′	(832–852)	531	50
		Anti-sense	5′-CACCACTATACTCTCAACCCAA-3′	(1342–1363)		
TLR7	NM016562	Sense	5′-AGTGTCTAAAGAACCTGG-3′	(2222–2239)	544	50
		Anti-sense	5′-CCTGGCCTTACAGAAATG-3′	(2749–2766)		
TLR8	NM016610	Sense	5′-CAGAATAGCAGGCGTAACACATCA-3′	(1909–1932)	639	56
		Anti-sense	5′-AATGTCACAGGTGCATTCAAAGGG-3′	(2522–2545)		
TLR9	NM017442	Sense	5′-GTGCCCCACTTCTCCATG-3′	(791–808)	259	50
		Anti-sense	5′-GGCACAGTCATGATGTTGTTG-3′	(1030–1050)		
TLR10	NM030956	Sense	5′-CTTTGATCTGCCCTGGTATCTC-3′	(2286–2307)	497	52
		Anti-sense	5′-AGCCCACATTTACGCCTATCCT-3′	(2783–2286)		
GAPDH	XM033263	Sense	5′-CCATCACCATCTTCCAGGAG-3′	(293–312)	575	60
		Anti-sense	5′-CCTGCTTCACCACCTTCTTG-3′	(849–868)		

ELISA. To quantify cytokine secretion, culture supernatants were harvested and the level of IL-6 and IL-8 was assayed by human cytokine-specific ELISA (Biosource, Camarillo, CA).

Real-time semi-quantitative PCR. This was performed on an ABI-prism 7700 (Applied Biosystems, Foster City, CA) according to a previously described protocol [27] and the manufacturer's instructions. Total cellular RNA extraction and the first cDNA synthesis were as described above. The primers and probes for human IFN-β, human molecules possessing ankyrin-repeats induced by LPS (MAIL), and human GAPDH were from Perkin-Elmer Applied Biosystems. Previously reported primer and TaqMan probes for human IL-6 and IL-8 were used. The primers for IL-6 were 5′-TGACAAACAAATT CGGTACATCCT-3′ and 5′- AGTGCCTCTTTGCTGCTTTCAC-3′; the TaqMan probe for human IL-6 was 5′-TTACTCTTGTTACA TGTCTCCTTTCTCAGGGCTG-3′ [28]. The primers for human IL-8 were 5′-GCGCCAACACAGAAATTATTGTAA-3′ and 5′-TTATGA ATTCTCAGCCCTCTTCAA-3′; the TaqMan probe for IL-8 was 5′-TTCTCCACAACCCTCTGCACCCAGTT-3′ [27]. The probes were synthesized by Perkin-Elmer Applied Biosystems. To amplify human IL-6, IL-8, IFN-β, MAIL, and GAPDH cDNA, PCR was performed in a 25-μl total volume that contained a 1 μl cDNA template in 2× TaqMan universal PCR master mix (Applied Biosystems) at 50 °C for 2 min and 95 °C for 10 min, followed by 40 cycles at 95 °C for 15 s and 60 °C for 1 min. The results were analyzed with sequence detection software (Applied Biosystems); the expression level of each mRNA was normalized to the expression of the human housekeeping gene GAPDH.

Data analysis. Data were expressed as means ± SE and evaluated by Student's *t* test using the Excel program.

Results

Expression of TLR3-specific mRNA in human corneal epithelium

We first examined whether human corneal epithelium expresses specific mRNA for TLRs 1–10. TLR-specific RT-PCR showed that mRNA from all but TLR8 was present in normal human corneal epithelium (Fig. 1). Among TLR-specific mRNA tested, TLR3 was expressed most intensely. When, as a positive control, we also subjected mRNA isolated from HPMC to RT-PCR, we found that these cells expressed TLRs 1–10. We then isolated, subcloned, and sequenced the PCR products. The obtained sequences were >95% identical with the known nucleotide sequences of human TLRs. Our findings suggest that while human corneal epithelium harbors messages for most TLRs, TLR3 is the one with the highest expression level. The expression of TLR3 was higher, while that of the other TLRs was lower, in human corneal epithelium than HPMC.

Primary HCEC express TLR3, but not TLR2 and TLR4, on the cell surface

Next we examined the cell-surface expression of TLR2, TLR3, and TLR4 on primary HCEC. While TLR3 was expressed on the surface of primary HCEC, TLR2 and TLR4 were not (Fig. 2). In positive controls, TLR2 and TLR4 were expressed on the cell surface of human peripheral blood monocytes and TLR3 was expressed on the cell surface of MRC-5 [29].

Primary HCEC respond to polyI:C but not LPS

Next we determined whether HCEC respond to polyI:C, a mimic of TLR3 ligand dsRNA. We first examined the production of inflammatory cytokines by primary HCEC stimulated with polyI:C and LPS. As

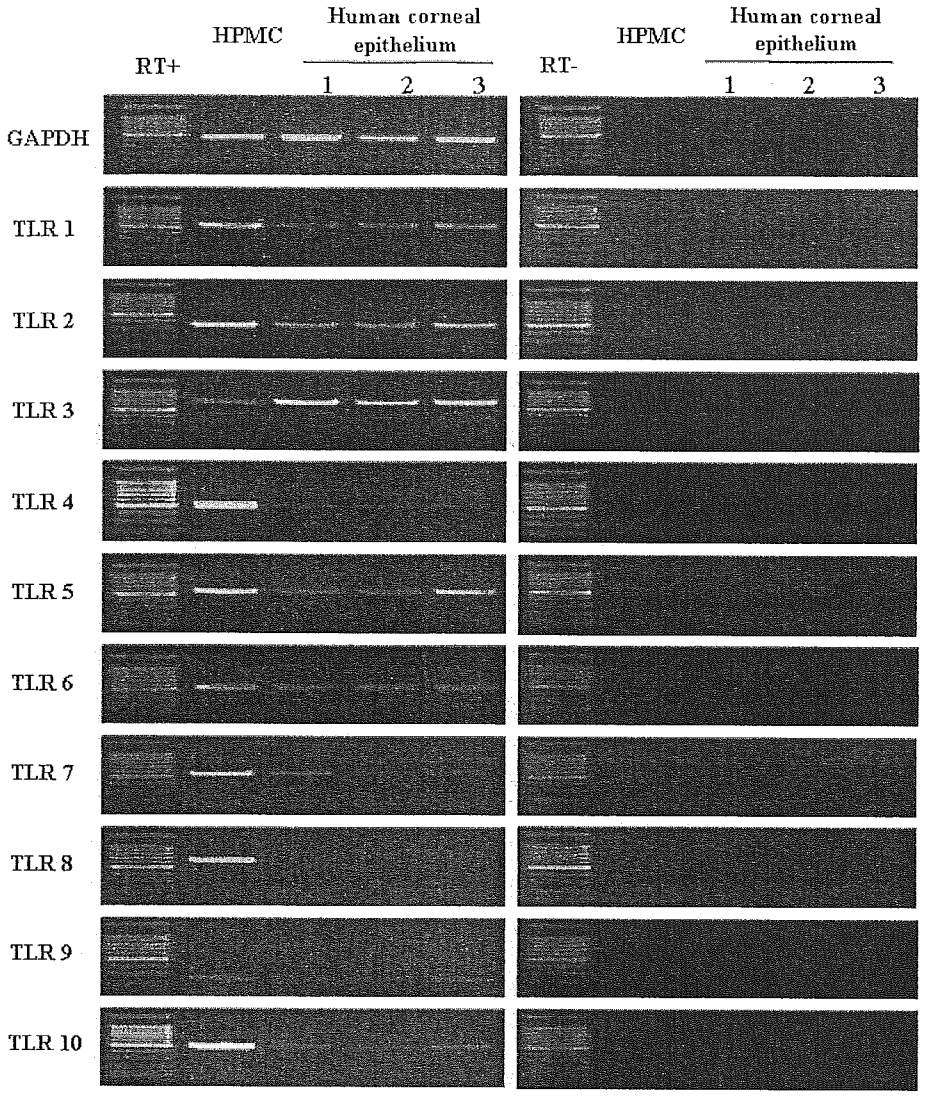

Fig. 1. The level of TLR3 expression is higher in human corneal epithelium than HPMC. Normal human corneal epithelium expresses mRNAs for TLRs 1–7 and 9–10 but not TLR8. As a positive control, mRNA isolated from human peripheral mononuclear cells (HPMC) was subjected to RT-PCR (left column). RT– indicates data were obtained without reverse transcription (controls).

shown in Fig. 3A, polyI:C stimulation induced the secretion of IL-6 and IL-8 while LPS treatment did not; in LPS-treated primary HCEC the level of IL-6 and IL-8 was similar to that seen in unstimulated cells. On the other hand, LPS stimulation significantly increased the production of IL-6 and IL-8 by HPMC and HCFB.

These findings were confirmed at the mRNA expression level. In primary HCEC, stimulation with polyI:C, but not LPS, resulted in the increased expression of IL-6- and IL-8-specific mRNA. Conversely, HPMC responded to LPS- but not to polyI:C stimulation and HCFB responded to both LPS and polyI:C (Fig. 3B).

IFN-β is controlled with TLR3/IRF-3 signaling. Thus, IFN-β-specific mRNA was significantly elevated in polyI:C- but not LPS-stimulated primary HCEC. Similarly, polyI:C but not LPS stimulated the induction of IFN-β in HPMC and HCFB. Surprisingly, IFN-β-specific mRNA expression was markedly higher in primary HCEC than HPMC and HCFB (Figs. 4A and B). Although primary human fibroblasts such as HCFB and MRC-5 expressed TLR3 on their cell surface, the cell-surface expression of TLR3 was more notable in primary HCEC (Fig. 4C).

Induction of IκBα- and MAIL-specific mRNA by polyI:C, but not LPS, in primary HCEC

In epithelial cells, the transcription factor NF-κB plays a central role in regulating genes that govern the onset of mucosal inflammatory responses. The primary consequences of TLR activation are NF-κB activation, cytokine secretion, and the expression of co-stimulatory molecules [9,30]. These responses help to promote and shape the critical immunological processes that facilitate

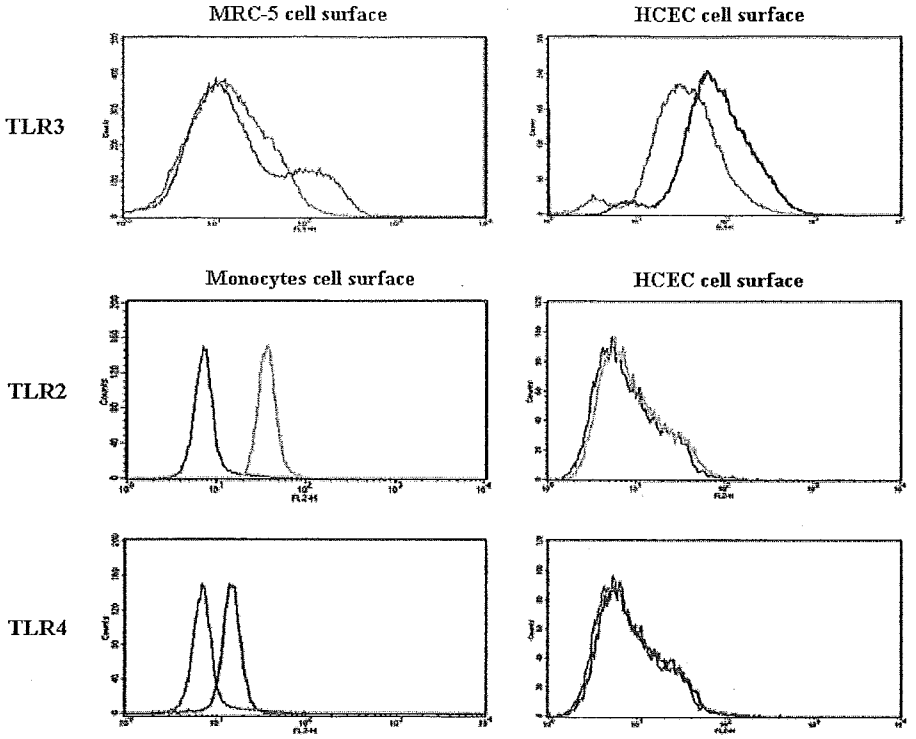

Fig. 2. Primary HCEC express TLR3, but not TLR2 and TLR4, on the cell surface. The cell-surface expression of TLR2, TLR3, and TLR4 was examined by flow cytometry. For TLR3 expression, cells were incubated (30 min, 4 °C) with mouse anti-human TLR3 monoclonal antibody or isotype control mouse IgG1. Alexa Fluor 488 goat anti-mouse IgG (H + L) was the secondary antibody. For TLR2 and TLR4 expression, cells were incubated (30 min, 4 °C) with PE-conjugated mouse anti-human TLR2 (TL2.1), TLR4 (HTA125) monoclonal antibody, or isotype control mouse IgG2a. The histogram data are representative of three separate experiments.

the control and clearance of pathogens. We examined whether polyI:C stimulation of primary HCEC induced mRNA specific for the IκB family, regulators of NF-κB, such as IκBα and MAIL. We found that the expression of IκBα- and MAIL-specific mRNA was in fact elevated by polyI:C but not LPS (Fig. 5). These mRNAs were not up-regulated in polyI:C-stimulated HPMC, but their expression was significantly up-regulated upon stimulation with LPS as described previously [31]. It is of note that MAIL-specific mRNA was elevated by both polyI:C and LPS in HCFB. Taken together, these findings show that polyI:C could up-regulate IκBα and MAIL expression in primary HCEC via TLR3 (Fig. 5).

PolyI:C stimulates the gene expression and surface expression of TLR3 in primary HCEC

In macrophages, high TLR3- but not TLR4 gene expression levels are induced by TLR3 and TLR4 agonists [32]. In the context of this autocrine loop of TLR3 expression, we examined whether TLR-specific mRNA was inducible in primary HCEC by the TLR3 agonist polyI:C. As shown in Fig. 6A, TLR3-specific mRNA was highly elevated in primary HCEC stimulated with polyI:C. Interestingly, increased TLR2 and TLR4 gene expression was also observed in polyI:C- but not LPS-stimulated primary HCEC. Furthermore, as shown in Fig. 6B, the cell-surface expression of TLR3, but not of TLR2 and TLR4, was increased. These observations raise interesting questions regarding the role of TLR3 in the host defense mounted by corneal epithelium.

Discussion

We provide evidence for the gene and surface expression of TLR3 in human corneal epithelium and suggest that expressed TLR3 is functionally active in the secretion of the inflammatory mediators IL-6, IL-8, and IFN-β. We thus documented that polyI:C can induce the secretion of inflammatory mediators by primary HCEC. The ability of IFN-β to prevent the death of anergic cells, in addition to its anti-proliferative effect, may be one way in which the immune system regains a quiescent state after activation [33]. Further studies are necessary to elucidate the pathological role of IFN-β produced by HCEC. It is noteworthy that TLR3 expression was up-regulated by the TLR3 agonist polyI:C. Furthermore, the up-regulation in primary HCEC of IκB-α and MAIL (a human homologue of IκBζ, a NF-κB regulator in the nucleus) by polyI:C suggests a

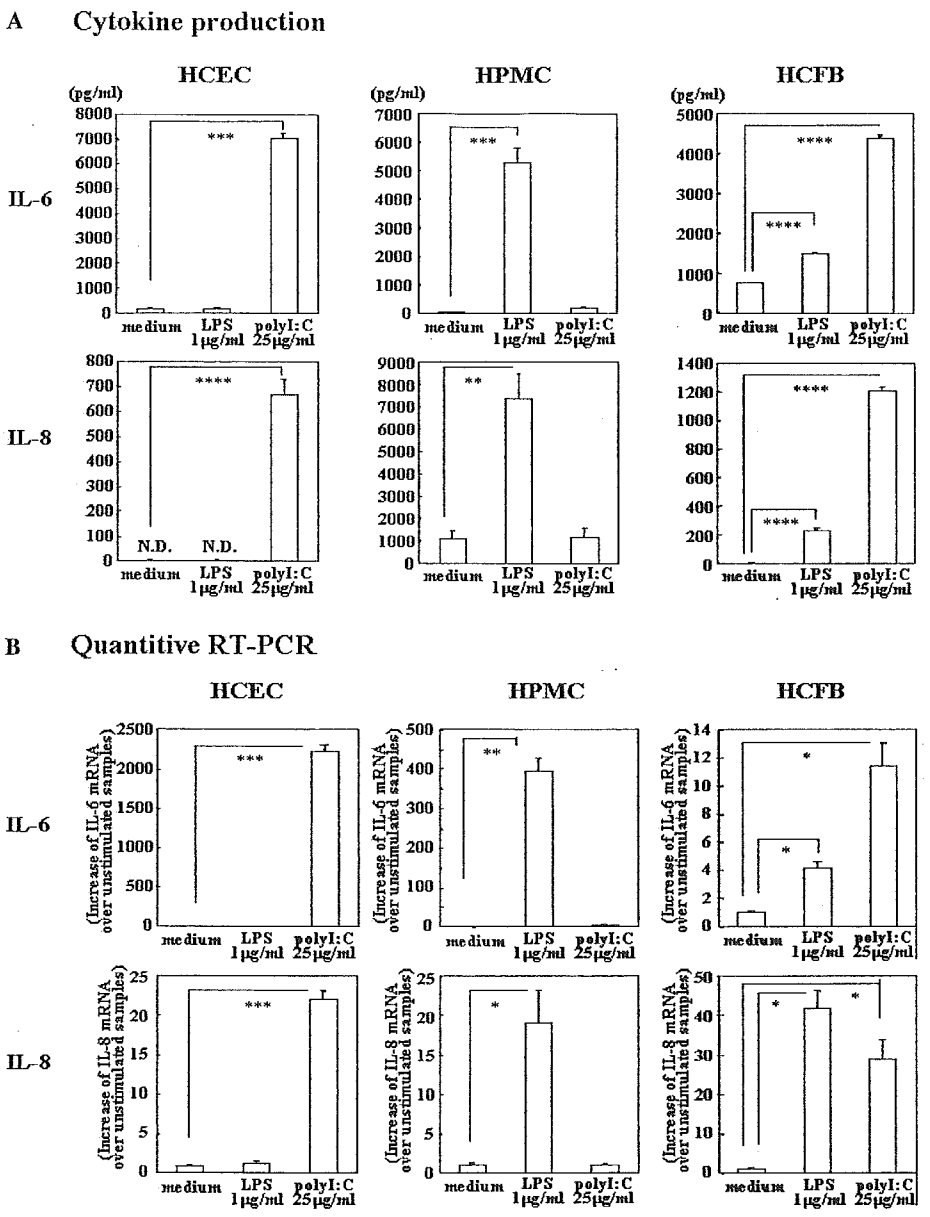

Fig. 3. The production and mRNA expression of IL-6 and IL-8 by primary HCEC. Primary HCEC and HCFB were cultured to sub-confluence and exposed to 1 μg/ml LPS from *P. aeruginosa* or 25 μg/ml polyI:C for 6 h. HPMC were cultured at a density of about 1×10^6 cells/ml and exposed to either 1 μg/ml LPS from *P. aeruginosa* or 25 μg/ml polyI:C for 6 h. (A) The culture supernatants were harvested and assayed by cytokine-specific ELISA for IL-6 and IL-8. (B) Total RNA was isolated from these cells with the Trizol reagent (Life Technologies). The RT reaction was performed with the SuperScript preamplification system (Invitrogen). Real-time semi-quantitative PCR was on an ABI-prism 7700. The *Y* axis shows the increase of specific mRNA over unstimulated samples. Data are representative of three separate experiments and show means ± SEM from an experiment carried out in triplicate wells ($*p < 0.05$; $**p < 0.01$; $***p < 0.005$; and $****p < 0.001$).

novel role for TLRs in ocular surface physiology. The new findings presented here contribute to a better understanding of innate ocular surface immunity.

A novel IκB protein, IκBζ/MAIL, induced by IL-1 and PAMPs regulates NF-κB in the cell nucleus. The induction of IκBζ is controlled by NF-κB, which, in turn, is negatively regulated by IκBζ, thereby forming an autonomous negative-feedback loop [34]. We postulate that IκBζ in ocular surface epithelium negatively regulates the pathological progression of ocular surface inflammation [35].

IκBζ was originally reported as a regulator of NF-κB induced by IL-1 and LPS [36]. LPS stimulation induced IκBζ in macrophages [31,34], but not primary HCEC (Fig. 4C). Furthermore, IκBζ is reportedly indispensable for IL-6 production in response to TLR ligands and is a positive regulator of NF-κB in the two-step process of IL-6 gene activation [37]. The implications of the

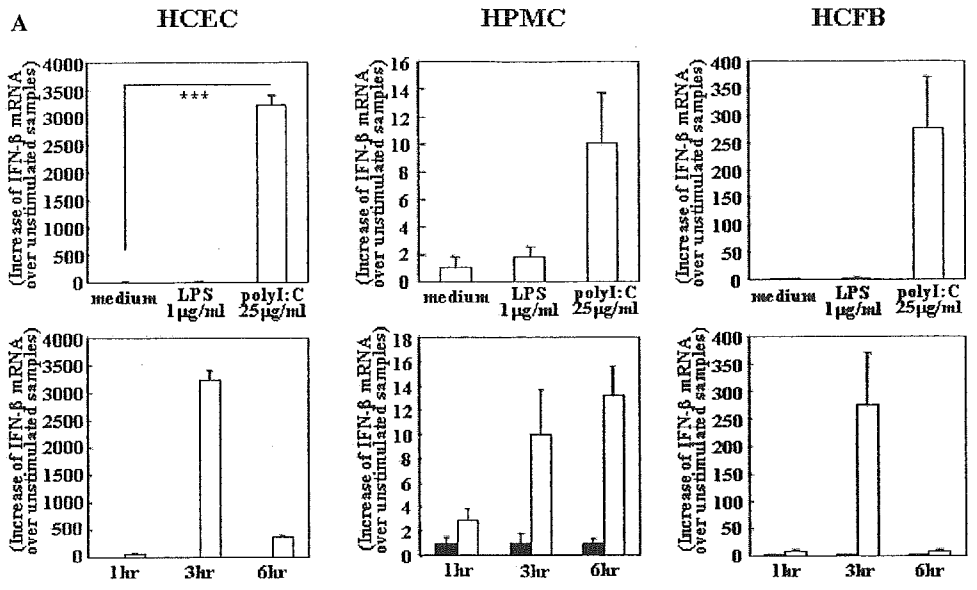

B The ratio of IFN-β/GAPDH mRNA at 3hr

	HCEC	ratio to HCEC	HPMC	ratio to HCEC	HCFB	ratio to HCEC	MRC-5	ratio to HCEC	HeLa	ratio to HCEC
unstimulated samples	0.00074 ±0.00014	1	0.01821 ±0.01295	24.6	0.00031 ±0.00002	4/10	0.00003 ±0.00002	4/100	0.0004 ±0.00013	5/10
stimulated with polyI:C	2.39136 ±0.13371	1	0.14682 ±0.06039	6/100	0.11038 ±0.01085	5/100	0.0462 ±0.00201	2/100	0.0468 ±0.00338	2/100
increasing ratio	3224	1	8	2/1000	360	1/10	1540	5/10	117	4/100

C Cell surface expression of TLR3

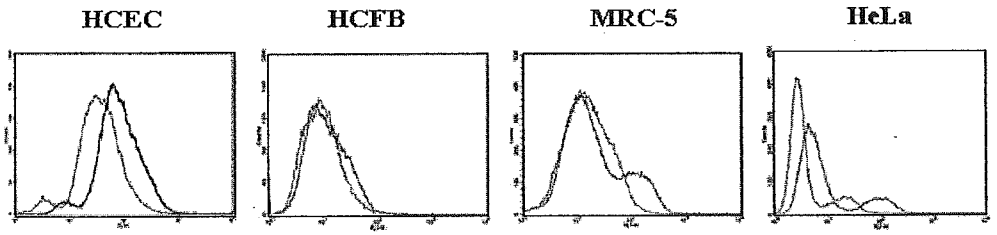

Fig. 4. Comparison of IFN-β mRNA expression and TLR3 cell-surface expression. (A) HCEC, HCFB, and HPMC were cultured as in Fig. 3 and exposed to either 1 μg/ml LPS from *P. aeruginosa* or 25 μg/ml polyI:C for 3 h. Subsequent procedures were as in the assay of mRNA expression. The *Y* axis shows the increase of specific mRNA over unstimulated samples. Data are representative of two separate experiments and show means ± SEM from an experiment carried out in triplicate wells (***$p < 0.005$). (B) The methods were as in (A). The actual ratio of IFN-β/GAPDH mRNA and the relative ratio in HCEC are summarized in the table. (C) Cell-surface expression of TLR3 was examined by flow cytometry. Cells were incubated (30 min, 4 °C) with mouse anti-human TLR3 monoclonal antibody or isotype control mouse IgG1. Alexa Fluor 488 goat anti-mouse IgG (H + L) was the secondary antibody. The histogram data are representative of three separate experiments.

induction by polyI:C of IκBζ/MAIL in primary HCEC remain to be determined.

The epithelial expression of TLRs may be of importance in inflammation and immunity in response to pathogens [38–41]. Unique patterns of TLR expression appear to exist at different host-environment tissue interfaces. Under physiological conditions, the corneal epithelium appears to be hyporesponsive to commensal bacteria to which it is consistently exposed. We previously reported that HCEC failed to respond functionally to LPS or PGN because they lack TLR2 and TLR4 on their cell surface [20]. Despite the presence of TLR2 and TLR4 in their cytoplasm, HCEC did not respond to experimentally translocated LPS [20]. This is indicative of a characteristic difference between HCEC and immune-competent cells such as macrophages. The selective expression of TLR3 in human corneal epithelium (Fig. 1) contrasts with the ubiquitous expression of TLR family members in HPMC and indicates that the regulation and localization of TLR3 are different

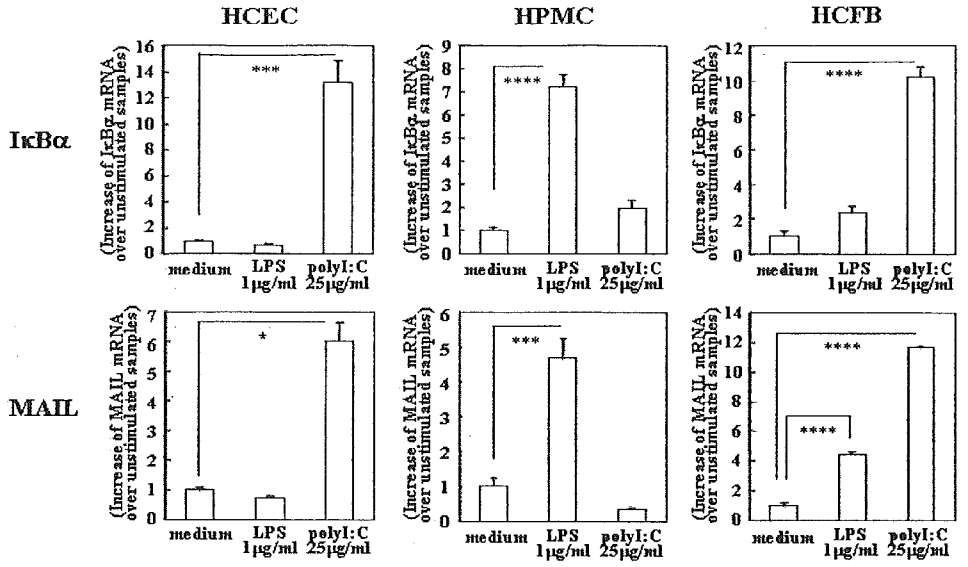

Fig. 5. Augmentation of MAIL and IκB-α gene expression in polyI:C-stimulated primary HCEC. HCEC, HCFB, and HPMC were cultured as in Fig. 3 and exposed to either 1 μg/ml LPS from *P. aeruginosa* or 25 μg/ml polyI:C for 3 h, subsequent procedures were as in the assay of mRNA expression. The *Y* axis shows the increase of specific mRNA over unstimulated samples. Data are representative of two separate experiments and show means ± SEM from an experiment carried out in triplicate wells ($*p < 0.05$; $***p < 0.005$; and $****p < 0.001$).

in these cells. This may reflect the participation of cell type-specific multiple pathways in antiviral IFN induction via TLR3 [42]. However, the previous work does not exclude the role of inflammation-dependent TLRs on HCEC or on antigen-presenting cells infiltrating corneal tissue. IFN-α up-regulated TLR3 mRNA expression in epithelial cells and IFN-γ enhanced TLR3 expression in epithelial- and endothelial cells [43]. In macrophages, TLR3 expression is inducible by both TLR3 and TLR4 ligands, although these stimuli fail to induce TLR4 expression. Furthermore, TLR3 and TLR4 require the IFN-β autocrine/paracrine feedback mechanism to induce TLR3 expression and to activate and/or enhance genes required for antiviral activity [32]. IFN-α/β is critical for the measles virus-mediated up-regulation of TLR3 induction [44]. Given that cell-surface TLR3 expression was up-regulated by an agonist of TLR3, polyI:C (Fig. 6), and that polyI:C was able to induce the gene expression of IFN-β in HCEC (Fig. 4B), it is conceivable that IFN-β is crucial for the innate immune response of the ocular surface to pathogenic and nonpathogenic viruses and bacteria.

LPS up-regulates TLR3 expression in murine phagocytic cells through autocrine IFN-β induction. In humans, however, the IFN-β-induced up-regulation of TLR3 was blocked by pretreatment with LPS [45]. This observation coincides with our present results that TLR3 expression was not up-regulated by an agonist of TLR4, LPS (Fig. 6), and that LPS was incapable of inducing the gene expression of IFN-β in HCEC (Fig. 4A). The species-specific differences between humans and mice in their responses to LPS coincide with the presence of different, evolutionary nonconserved promoter sequences in both species. The intriguing functionality of TLR3 in HCEC and the far more potent induction of IFN-β by a TLR3 agonist in HCEC than fibroblasts require elucidation of the molecular mechanisms that regulate TLR3 expression on HCEC.

Although all TLRs activate NF-κB, not all TLRs activate IRF3 or induce IFN-β expression. TLR3 and TLR4 are the best-characterized TLRs known to activate IRF3 [30]. The TIR domain-containing adapter-inducing IFN-β (TRIF) is also an adapter for TLR3 and TLR4 [46,47]. Unlike the other TLRs including TLR4 that use the common MyD88-dependent pathway, TLR3 seems to employ only MyD88-independent TRIF-dependent pathways. These biochemical findings may account for the distinctly different responses elicited by polyI:C and LPS in the present study.

Type I IFN is induced not only by viral but also by bacterial infection [22,48]. An understanding of the role of the TLR3-IFN-β-link is crucial for understanding the involvement of type I IFN in TLR3-induced biological effects on the ocular surface. O'Conell et al. [49] reported that type I IFNs play a different role in bacterial and viral infections. The sophisticated interplay between bacteria and viruses may culminate in the exacerbation of pathological inflammation on the ocular surface.

In summary, the innate immune responses in mucosal epithelial cells such as HCEC differ from those in immune-competent cells such as macrophages. The elucidation of the unique innate immune response in mucosal epithelium is critical for a better understanding of the symbiotic relationship between mucosal epithelial cells and commensal bacteria inhabiting the mucosal surface.

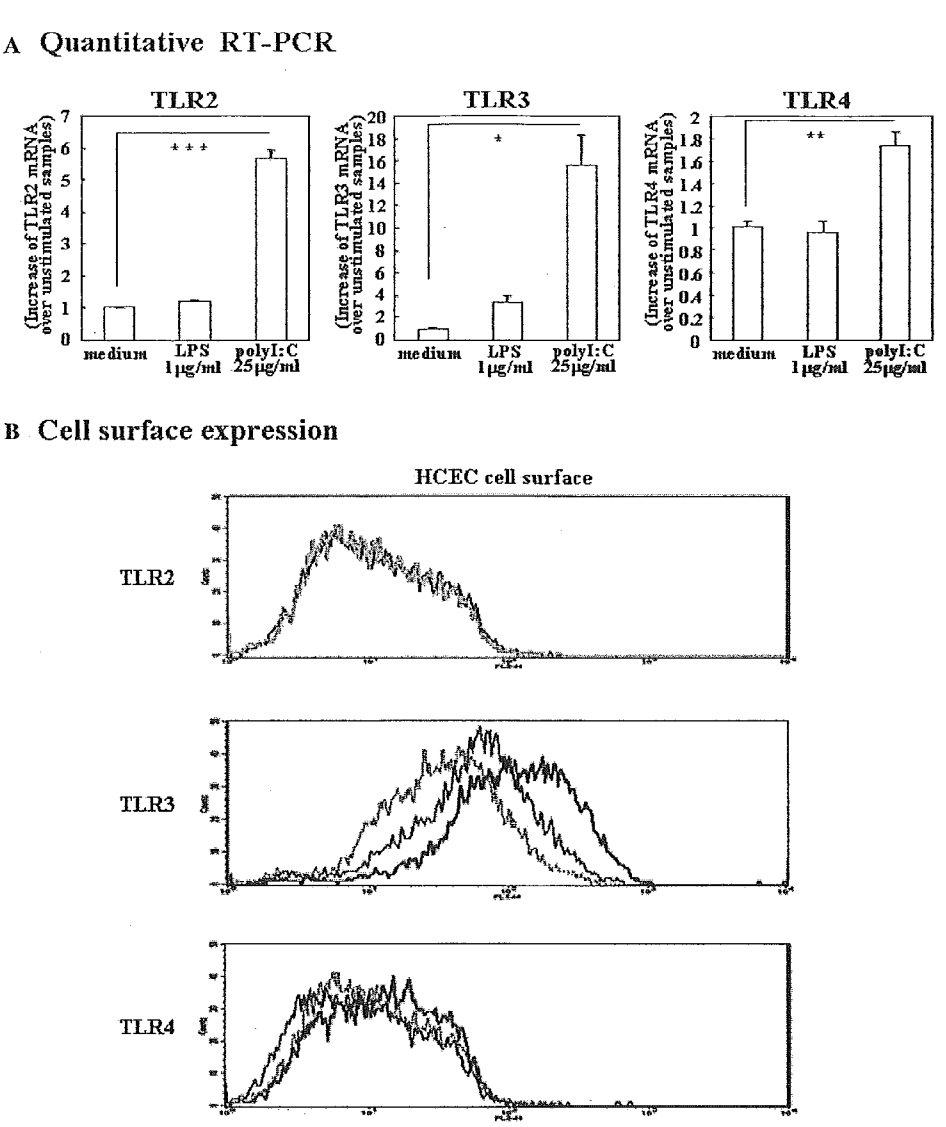

Fig. 6. Augmentation of TLR3 expression on HECE by polyI:C stimulation. (A) Augmentation of TLR3 gene expression in polyI:C-stimulated primary HCEC. Primary HCEC were cultured to sub-confluence in 25 cm^2 flasks (2×10^6 cells/flask) and exposed to 1 μg/ml LPS from *P. aeruginosa* or 25 μg/ml polyI:C for 6 h. RNA extraction, RT reaction, and real-time semi-quantitative PCR were as in Fig. 3. The *Y* axis shows the increase of specific mRNA over unstimulated samples. Data are representative of three separate experiments and show means ± SEM from an experiment carried out in triplicate wells. (B) Augmentation of TLR3 cell-surface expression on polyI:C-stimulated primary HCEC. Primary HCEC were cultured to sub-confluence in 75 cm^2 flasks (6×10^6 cells/flask) and untreated or exposed to 25 μg/ml polyI:C for 6 h. The cell-surface expression of TLR2, TLR3, and TLR4 was examined by flow cytometry. For TLR3 expression, cells were incubated (30 min, 4 °C) with mouse anti-human TLR3 monoclonal antibody or isotype control mouse IgG1. Alexa Fluor 488 goat anti-mouse IgG (H + L) was the secondary antibody. For TLR2 and TLR4 expression, cells were incubated (30 min, 4 °C) with PE-conjugated mouse anti-human TLR2 (TL2.1), TLR4 (HTA125) monoclonal antibody, or isotype control mouse IgG2a. The histogram data are representative of two separate experiments (dotted line, isotype control; thin line, untreated; and bold line, stimulated with 25 μg/ml polyI:C for 6 h).

Acknowledgments

This work was supported in part by Grants-in-Aid for scientific research from the Japanese Ministry of Health, Labour and Welfare, the Japanese Ministry of Education, Culture, Sports, Science and Technology, CREST from JST, a research grant from the Kyoto Foundation for the Promotion of Medical Science, and the Intramural Research Fund of Kyoto Prefectural University of Medicine. We thank Dr. T. Seya and Dr. J. Yamada for the gift of MRC5, HeLa cells, and HCFB, respectively, and Ms. C. Mochida for her technical assistance.

References

[1] R.J. Haynes, P.J. Tighe, H.S. Dua, Br. J. Ophthalmol. 83 (1999) 737–741.
[2] J.W. Streilein, Nat. Rev. Immunol. 3 (2003) 879–889.

[3] J.M. Williams, M.E. Fini, S.W. Cousins, J.S. Repose, in: J.H. Krachmer, M.J. Mannis, E.J. Holland (Eds.), Cornea, Mosby, St. Louis, 1997, pp. 128–162.
[4] G. Bouma, W. Strober, Nat. Rev. Immunol. 3 (2003) 521–533.
[5] W. Strober, Nat. Med. 10 (2004) 898–900.
[6] W. Strober, I.J. Fuss, R.S. Blumberg, Annu. Rev. Immunol. 20 (2002) 495–549.
[7] R. Medzhitov, P. Preston-Hurlburt, C.A. Janeway Jr., Nature 388 (1997) 394–397.
[8] M. Schnare, G.M. Barton, A.C. Holt, K. Takeda, S. Akira, R. Medzhitov, Nat. Immunol. 2 (2001) 947–950.
[9] K. Takeda, T. Kaisho, S. Akira, Annu. Rev. Immunol. 21 (2003) 335–376.
[10] V. Hornung, S. Rothenfusser, S. Britsch, A. Krug, B. Jahrsdorfer, T. Giese, S. Endres, G. Hartmann, J. Immunol. 168 (2002) 4531–4537.
[11] D. Zhang, G. Zhang, M.S. Hayden, M.B. Greenblatt, C. Bussey, R.A. Flavell, S. Ghosh, Science 303 (2004) 1522–1526.
[12] S.E. Girardin, P.J. Sansonetti, D.J. Philpott, Trends Microbiol. 10 (2002) 193–199.
[13] N. Inohara, G. Nunez, Nat. Rev. Immunol. 3 (2003) 371–382.
[14] C.A. Leifer, M.N. Kennedy, A. Mazzoni, C. Lee, M.J. Kruhlak, D.M. Segal, J. Immunol. 173 (2004) 1179–1183.
[15] M. Kurpakus-Wheater, K.A. Kernacki, L.D. Hazlett, Prog. Histochem. Cytochem. 36 (2001) 185–259.
[16] K.A. McClellan, Surv. Ophthalmol. 42 (1997) 233–246.
[17] M.I. Aswad, T. John, M. Barza, K. Kenyon, J. Baum, Ophthalmology 97 (1990) 296–302.
[18] O.G. Gudmundsson, L.D. Ormerod, K.R. Kenyon, R.J. Glynn, A.S. Baker, J. Haaf, S. Lubars, M.B. Abelson, S.A. Boruchoff, C.S. Foster, et al., Cornea 8 (1989) 115–121.
[19] D.J. Philpott, S.E. Girardin, P.J. Sansonetti, Curr. Opin. Immunol. 13 (2001) 410–416.
[20] M. Ueta, T. Nochi, M.H. Jang, E.J. Park, O. Igarashi, A. Hino, S. Kawasaki, T. Shikina, T. Hiroi, S. Kinoshita, H. Kiyono, J. Immunol. 173 (2004) 3337–3347.
[21] L. Alexopoulou, A.C. Holt, R. Medzhitov, R.A. Flavell, Nature 413 (2001) 732–738.
[22] K. Hoshino, T. Kaisho, T. Iwabe, O. Takeuchi, S. Akira, Int. Immunol. 14 (2002) 1225–1231.
[23] A. Poltorak, X. He, I. Smirnova, M.Y. Liu, C. Van Huffel, X. Du, D. Birdwell, E. Alejos, M. Silva, C. Galanos, M. Freudenberg, P. Ricciardi-Castagnoli, B. Layton, B. Beutler, Science 282 (1998) 2085–2088.
[24] P.M. Pitha, Proc. Natl. Acad. Sci. USA 101 (2004) 695–696.
[25] M. Prialnick, O. Smetana, N. Kariv, H. Savir, E. Eylan, Ann. Ophthalmol. 20 (1988) 439–443.
[26] O. Smetana, E. Eylan, N. Kariv, Med. Microbiol. Immunol. (Berl.) 171 (1982) 99–112.
[27] H.H. Tong, Y. Chen, M. James, J. Van Deusen, D.B. Welling, T.F. DeMaria, Infect. Immun. 69 (2001) 3678–3684.
[28] E.J. Birks, N. Latif, V. Owen, C. Bowles, L.E. Felkin, A.J. Mullen, A. Khaghani, P.J. Barton, J.M. Polak, J.R. Pepper, N.R. Banner, M.H. Yacoub, Circulation 104 (2001) I233–I240.
[29] M. Matsumoto, S. Kikkawa, M. Kohase, K. Miyake, T. Seya, Biochem. Biophys. Res. Commun. 293 (2002) 1364–1369.
[30] S. Akira, K. Takeda, Nat. Rev. Immunol. 4 (2004) 499–511.
[31] S. Yamazaki, T. Muta, K. Takeshige, J. Biol. Chem. 276 (2001) 27657–27662.
[32] S.E. Doyle, R. O'Connell, S.A. Vaidya, E.K. Chow, K. Yee, G. Cheng, J. Immunol. 170 (2003) 3565–3571.
[33] G. Lombardi, P.J. Dunne, D. Scheel-Toellner, T. Sanyal, D. Pilling, L.S. Taams, P. Life, J.M. Lord, M. Salmon, A.N. Akbar, J. Immunol. 165 (2000) 3782–3789.
[34] A. Eto, T. Muta, S. Yamazaki, K. Takeshige, Biochem. Biophys. Res. Commun. 301 (2003) 495–501.
[35] M. Ueta, J. Hamuro, M. Yamamoto, K. Kaseda, S. Akira, S. Kinoshita, Invest. Ophthalmol. Vis. Sci. 46 (2005) 579–588.
[36] H. Kitamura, K. Kanehira, K. Okita, M. Morimatsu, M. Saito, FEBS Lett. 485 (2000) 53–56.
[37] M. Yamamoto, S. Yamazaki, S. Uematsu, S. Sato, H. Hemmi, K. Hoshino, T. Kaisho, H. Kuwata, O. Takeuchi, K. Takeshige, T. Saitoh, S. Yamaoka, N. Yamamoto, S. Yamamoto, T. Muta, K. Takeda, S. Akira, Nature 430 (2004) 218–222.
[38] M.T. Abreu, P. Vora, E. Faure, L.S. Thomas, E.T. Arnold, M. Arditi, J. Immunol. 167 (2001) 1609–1616.
[39] M.N. Becker, G. Diamond, M.W. Verghese, S.H. Randell, J. Biol. Chem. 275 (2000) 29731–29736.
[40] E. Cario, D.K. Podolsky, Infect. Immun. 68 (2000) 7010–7017.
[41] J. Zhang, K. Xu, B. Ambati, F.S. Yu, Invest. Ophthalmol. Vis. Sci. 44 (2003) 4247–4254.
[42] M. Matsumoto, K. Funami, M. Tanabe, H. Oshiumi, M. Shingai, Y. Seto, A. Yamamoto, T. Seya, J. Immunol. 171 (2003) 3154–3162.
[43] M. Miettinen, T. Sareneva, I. Julkunen, S. Matikainen, Genes Immun. 2 (2001) 349–355.
[44] M. Tanabe, M. Kurita-Taniguchi, K. Takeuchi, M. Takeda, M. Ayata, H. Ogura, M. Matsumoto, T. Seya, Biochem. Biophys. Res. Commun. 311 (2003) 39–48.
[45] S. Heinz, V. Haehnel, M. Karaghiosoff, L. Schwarzfischer, M. Muller, S.W. Krause, M. Rehli, J. Biol. Chem. 278 (2003) 21502–21509.
[46] H. Oshiumi, M. Matsumoto, K. Funami, T. Akazawa, T. Seya, Nat. Immunol. 4 (2003) 161–167.
[47] M. Yamamoto, S. Sato, K. Mori, K. Hoshino, O. Takeuchi, K. Takeda, S. Akira, J. Immunol. 169 (2002) 6668–6672.
[48] C. Bogdan, Curr. Opin. Immunol. 12 (2000) 419–424.
[49] R.M. O'Connell, S.K. Saha, S.A. Vaidya, K.W. Bruhn, G.A. Miranda, B. Zarnegar, A.K. Perry, B.O. Nguyen, T.F. Lane, T. Taniguchi, J.F. Miller, G. Cheng, J. Exp. Med. 200 (2004) 437–445.